Hair follicle renewal: organization of stem cells in the matrix and the role of stereotyped lineages and behaviors

Emilie Legué and Jean-François Nicolas*

Unité de Biologie moléculaire du Développement, Institut Pasteur, 25 rue du Docteur Roux, 75724 Paris Cedex 15, France
*Author for correspondence (e-mail: jfnicola@pasteur.fr)

Accepted 11 July 2005

Development 132, 4143-4154
Published by The Company of Biologists 2005
doi:10.1242/dev.01975

Summary

Hair follicles (HFs) are renewed via multipotent stem cells located in a reservoir (the bulge); however, little is known about how they generate multi-tissue HFs from a proliferative zone (the matrix). To address this issue, we temporally induced clonal labeling during HF growth. Challenging the prevailing hypothesis, we found that the matrix contains restricted self-renewing stem cells for each inner structure. These cells are located around the dermal papilla forming a germinative layer. They occupy different proximodistal sectors and produce differentiated cells along the matrix radial axis via stereotyped lineages and cell behavior. By contrast, the outer layer of HFs displays a mode of growth involving apoptosis that coordinates the development of outer and inner structures. HF morphology is therefore determined by the organization of cell fates along the proximodistal axis and by cell behavior along the radial (lateral) axis in the matrix. Thus, our studies suggest that fate and behavior are organized by two systems (uncoupled), and this uncoupling may represent a fundamental way to simplify morphogenesis.

Key words: Stem cell, Hair follicle, Morphogenesis, Cell lineage, Cell behavior, Clonal analysis, Mouse, Temporally induced clones, Apoptosis, Anagen, Cell competition, Developmental strategy

Introduction

The hair follicle (HF) is a fascinating model of morphogenesis (Fuchs et al., 2001; Hardy, 1992). Like complex embryonic systems, its formation involves multipotent cells producing differentiated cell types, which are spatially arranged to generate a multi-tissue structure. The HF also has the following features that make it an ideal model for studying the relationship between developmental genes and morphogenesis: (1) it displays cyclic renewal (Stenn and Paus, 2001), with each cycle initiated from multipotent stem cells (Cotsarelis et al., 1990; Morris et al., 2004; Oliver, 1966; Oshima et al., 2001; Tumbar et al., 2004); (2) in mice, a new cycle is initiated every four weeks throughout the life of the animal; (3) there are 150,000 synchronizable HFs; and (4) the structure formed remains simple; the number of cells involved is small and the renewal process is slow. These characteristics open up various possibilities for experimentation.

Recent advances in our understanding of HF renewal have provided insights into key questions in morphogenesis. It has been demonstrated that some of the major operations of development, such as cell proliferation and differentiation, cell signaling and cell rearrangements, are involved in HF renewal. Importantly, these operations are precisely orchestrated. It is therefore not surprising that almost all signaling pathways involved in embryogenesis have also been shown to be involved in HF renewal. These include *Shh* (Oro and Higgins, 2003), Wnt genes (Alonso and Fuchs, 2003), Bmp genes (Botchkarev, 2003; Kulessa et al., 2000), Fgf genes (Petiot et al., 2003), Notch family members and their ligands (Pan et al., 2004), together with many transcription factors [e.g. *Lef1/Tcf* (Merrill et al., 2001), *Krox20* (Gambardella et al., 2000), *Gata3* (Kaufman et al., 2003), and *Msx1* and *Msx2* (Ma et al., 2003)] as well as some belonging to the Hox complex (*Hoxc12* and *Hoxc13*) (Shang et al., 2002).

The HF comprises several concentric epithelial structures. The medulla, the cortex and the cuticle form the hair shaft, which is enveloped by two epithelial sheaths, known as the inner root sheath (IRS) and the outer root sheath (ORS). At the distal end of the HF, IRS cells undergo apoptosis (Tobin et al., 2002) and liberate the hair shaft. The matrix is a proliferative zone located at the proximal end of the HF surrounding the dermal papilla (DP). With the exception of the ORS, all cells are produced by the matrix. In HF renewal, morphogenesis occurs during anagen, a period following normal or induced HF destruction. Morphogenesis follows, resulting in the generation of a multi-tissue structure.

Several molecules (Msx1 and Msx2, Ptc1) are expressed uniformly throughout the matrix (Ma et al., 2003; Oro and Higgins, 2003), whereas others have a restricted expression pattern (Shh, Krox20, type II receptor of TGF β) (Gambardella et al., 2000). Lef1 and P-cadherin are expressed only in the cell layers near the DP, whereas E-cadherin is expressed in the more external layers (Jamora et al., 2003). However, the expression patterns of developmental genes have not yet identified distinct cell populations within the matrix involved in producing the different layers. The prevalent hypothesis is that the matrix is primarily a structure in which multipotent (Kopan et al., 2002) cells proliferate, perhaps owing to the control of BMP levels (Kulessa et al., 2000). When cells leave this structure they acquire their final identity (Niemann and

Watt, 2002), according to their position (Kulessa et al., 2000). In accordance with this model, labeling with Ki67 (Kobielak et al., 2003), BrdU (Oshima et al., 2001) and tritiated thymidine (Epstein and Maibach, 1965) has demonstrated that the cells of the matrix proliferate and specific biochemical markers (Gata3, keratins) have been detected in different layers, starting just above the bulb (Kaufman et al., 2003; Kobielak et al., 2003). However, this view is not supported by other observations. For example, mice expressing Noggin ectopically in the matrix have a defect specific to hair shaft cells (Kulessa et al., 2000); skin reconstitution assays (Kamimura et al., 1998), as well as retroviral labeling (Ghazizadeh and Taichman, 2001), have suggested the existence of one progenitor cell for hair shaft lineages and one for the inner root sheath lineages.

These discrepancies highlight the need to determine how cells are organized in the matrix. The key questions are whether the matrix is simply a zone of multipotent proliferating cells or of several cell populations, and whether these populations in the matrix are spatially organized (Langbein and Schweizer, 2005). Correct interpretation of the roles of developmental genes and signaling molecules depends on this knowledge.

We investigated cellular organization in the matrix by carrying out an extensive clonal analysis of HF morphogenesis during anagen. We developed a novel method of clonal analysis based on the temporal induction of β-galactosidase labeling. This method exploits a Cre-LoxP system, in which a Cre recombinase fused to a mutated estrogen receptor responds specifically to hydroxytamoxifen (OHT), this fusion is under the control of a CMV promoter in a Cre inducible mouse line CMV Cre ER^T (Feil et al., 1996). Rosa 26 reporter mice (R26R) (Soriano, 1999) were used to detect the recombination in Cre-targeted cells and their descendants. In CMV Cre ER^T×R26R F1, the *lacZ* gene is not transcribed. Hydroxytamoxifen (OHT), which binds to the ER^T, induces Cre nuclear translocation and therefore excision of the LoxP flanked stop sequence, allowing *lacZ* transcription and leading to an inheritable labeling (Fig. 1A).

Our results challenge the hypothesis that the matrix contains equivalent multipotent cells. We show that matrix cells display a highly sophisticated organization and carry out several functions controlling the shape of the HF. The inner structures are each produced by a distinct, restricted set of precursors occupying a specific position along the proximodistal axis of the matrix. These cells are capable of self-renewal and produce transient progenitors, and they therefore have attributes of stem cells. By contrast, the ORS displays a regional mode of growth, being generated by progenitors that divide locally. Based on these results, we draw a detailed map of the fate and behavior of the cells of the matrix and propose a new model of HF morphogenesis. This fate map should help us to understand the genetic basis of HF morphogenesis and the cellular operations involved. The simplicity of the HF and our precise knowledge of the genes involved in generating this structure make the HF a highly attractive model for studying the process of morphogenesis in higher vertebrates.

Materials and methods

Transgenic mouse lines

In CMV Cre ER^T line, provided by Daniel Metzger (Feil et al., 1996), Cre recombinase is fused to the modified estrogen receptor ER^T and is under the transcriptional control of the enhancer/promoter region of the major IE gene of human cytomegalovirus (CMV) that confers expression in a wide range of tissues, including the skin and its derivatives. The R26R Cre reporter mouse, was provided by Philippe Soriano (Soriano, 1999). The ROSA26 promoter confers ubiquitous expression on *lacZ*. These two lines were crossed and double-homozygous animals generated. Double homozygous males were crossed with wild-type B6D2 females to generate animals that were selected after checking for the absence of β-galactosidase$^+$ cells by skin biopsy on P30. The a-EGFP-F line, which expresses a farnesylated-GFP, was provided by Alexander Medvinsky. The GATA3 nls *lacZ* line was provided by Franck Grosveld (Hendriks et al., 1999).

Synchronization of HF cycles

HF cycles were synchronized in a large area on the back of the mice by depilation with cold wax. Depilation was performed on 6- to 8-week-old mice whose HFs were mostly in telogen. The areas that were in anagen regrew very rapidly and were not sampled. Depilation of telogen HFs mimicks exogen and induces synchronously the initiation of anagen in all depilated HFs (Stenn and Paus, 2001).

Production of temporally induced β-galactosidase$^+$ clones

In vivo, labeling was initiated by intraperitoneal injection of OHT (67 μg/g), in CMV Cre ER^t × R26R F1 mice, which gave 80-90% unlabelled HFs. Most labeling was therefore clonal in origin. On the day of the injection, a skin biopsy was sampled to determine the stage of the HF at the time of induction (Muller-Rover et al., 2001).

Treatment of biopsy samples

Pieces of skin were removed from anesthetized mice, fixed 20 minutes in 4% PFA-PBS at 4°C then washed three times in PBS. Fat and muscles were carefully removed with fine forceps, and biopsy samples were then incubated in X-gal staining solution.

HF description

HFs were carefully dissected with fine forceps under a dissecting microscope, screened and examined in toto for β-galactosidase$^+$ cells at 60× magnification. The low frequency of labeling in the HF demonstrates that most labeled cells were derived from a single recombination event. The frequency of two independent events is equal to the product of the probability of each single event. Thus, the calculated number of observations of two independent events is C=N*N/Nt where N is the number of observation of events and Nt the total number of observations. For example, the animal in which the frequency of labeling is the highest (animal 2), N=51, Nt=225, C=11.56, the probability of more than one recombination event in the same HF (C/Nt) is 5.1×10^{-2}. Each HF was classified, and photographed and a digital library of the clones was produced. a-EGFP-F HFs were observed with a confocal microscope (Zeiss Axiovert 200M) and images were obtained and processed with LSM510 software. We studied the awl and zig-zag HF categories.

Immunostaining

Cleaved caspase 3 immunostaining was performed as described previously (Kassar-Duchossoy et al., 2005).

Nomenclature

We define progenitor cells here as the cells for which all descendants contribute to a single structure and have a limited potential of division. We define permanent precursor cells as the cells that can divide during an entire HF cycle. We define coherent growth as a mode of growth during which cells remain close together after division. Founder cells of a structure are the earliest cells of which all descendants participate in the structure (Petit et al., 2005).

Results

Experimental plan

We synchronized HF renewal on an area where HFs were in telogen on the back of a mouse by local depilation. The HFs in this area initiate a new anagen phase (Stenn and Paus, 2001). Three days after depilation, the matrix organizes itself around the DP. The HFs then grow linearly (Fig. 1C) at least until D14. Thus, this period is convenient to analyze HF growth. Two weeks after depilation (D14), the labeled cells of the HF are identifiable based on morphology and position (Fig. 1D). The medulla cells are filled with melanin granules (Fig. 1D,E) and are encased by cortex cells that are elongated along the proximodistal axis (Fig. 1D,F). The cuticle cells have a distinctive ring shape (Fig. 1D,G) and are adjacent to the GATA3-positive inner root sheath (IRS) cells (Kaufman et al., 2003) (Fig. 1K). IRS cells are tile-shaped and occupy the layer adjacent to the ORS (Fig. 1D,H). GATA3 expression (Fig. 1K) restricted to the IRS (Kaufman et al., 2003) confirmed our identification of IRS cells. ORS cells form the most external layer of the HF and exhibit two types of morphology: small and elongated along the HF circumference (Fig. 1I) or large and round (Fig. 1J). We also observed melanoblasts and melanocytes, but did not study them because their lineage is unrelated to that of the integument. The different cell types are recognizable at D14, we chose it as the reference point for the analysis of the composition of the clones.

Restricted precursors at the origin of the different structures of the HF

In experiment 1 (Fig. 1B), clonal labeling is induced 8 days after depilation, by injecting OHT into CMV Cre $ER^T \times$ R26R F1 mice and HFs are observed on D14. We found that all HF structures were labeled, indicating that all structures were accessible at D8. The most striking observation is that most clones (101 of 130) contribute to only one structure: the cortex and cuticle [referred to as 'cuticle clones' as they share common clonal origin and molecular markers such as AE13 (Kaufman et al., 2003)], the medulla, the IRS or the ORS (Table 1, simple labeling). HF growth during anagen therefore involves independent restricted precursor cells generating the medulla, the cuticle, the IRS or the ORS. ORS clones are the most frequent (75/100). Composite labeling was also observed (n=29, combined+complex labeling, Table 1), frequently involving a combination of the ORS (combined labeling, 14 out of 29 cases) and another structure. Statistical analysis (composed probabilities) suggested that combined labeling corresponded to independent labeling events. The composed probability is the product of the frequency of each single event. We can approximate the frequency of labeling of the ORS by $f_O=(N_O+N_{OIm}+N_{OCm}+N_{OICm}+N_{OIC}+N_{OImCm}+N_{OImC})/Nt$ and of the IRS by $f_I=(N_{Im}+N_I+N_{OI}+N_{OIm}+N_{IC}+N_{imCm}+N_{imC}+N_{cmI}+N_{OIC}+N_{OImCm}+N_{OImC})/Nt$. Thus, the calculated frequency for a double event of labeling in ORS and IRS is $f_{OI}=f_O* f_I$. For

Table 1. Categories of labeled D14 HF induced at D8 or D11 after depilation

	D8 (experiment 1)				D11 (experiment 2)	
	Animal 1	Animal 2	Animal 3	Total D8	Animal 1	
Total	1291	225	239		495	
Labeled HF	181	51	57		157	
% of labeled HF	14	22.7	21.9		26.4	
Analyzed HF	69	25	36	130	77	
Simple labeling						
O, Om	44	9	22	75	34	
I	0	0	0	0	3	
C	0	0	0	0 (1)	5	(10)
M	nd	1	0	1	2	
Im	10	2	1	13	5	
Cm	5	3	1	9 (25)	1	(7)
Mm	nd	2	1	3	1	
Combined labeling						
O I	0	1	0	1	7	
O C	0	0	0	0 (2)	6	(14)
O M	nd	1	0	1	1	
O Im	3	3	3	9	6	
O Cm	1	1	0	2 (12)	2	(9)
O Mm	nd	0	1	1	1	
Complex labeling						
I C	0	0	1	1	0	
Im Cm	2	1	2	5	0	
Im C	0	1	1	2	1	
Cm I	0	0	1	1 (15)	0	(3)
O I C	2	0	0	2	1	
O Im Cm	2	0	0	2	1	
O Im C	0	0	2	2	0	

The HF grows from restricted precursors during anagen. Labeling categories in experiments 1 and 2. O, ORS; I, IRS; C, cuticle; M, medulla; m, matrix; O, I, C and M are categories in which the labeled cells are restricted to O, I, C and M. Im, Cm and Mm are labeled cells in I, C and M associated with labeled cells in the matrix. The other categories are combinations of these elementary categories. Total ' refers to the total number of observed HF (labeled + unlabeled); 'Labeled HF' is the number of observed labeled HF; 'Analyzed HF' is the number of HF that could be analyzed after dissection. Most clones (77.5%) are restricted to a single structure, demonstrating that most precursors are restricted during anagen.

example, in animal 1, the calculated f_{OIm}=(44+3+1+2+2)/492*(10+3+2+2+2)/492=0.41% is close to the observed f_{OIm} (i.e. 3/492=0.61%) showing that these clones are probably issued from two independent events of labeling.

In summary, this experiment demonstrates that during anagen, there are at least four populations of restricted precursors. This defines four clonal structures including the ORS, IRS, cuticle (cortex+cuticle) and medulla.

Restricted precursor cells display self-renewal and are located in the matrix

Growth of the inner structures of the HF depends on matrix cells. If the restricted precursors from inner

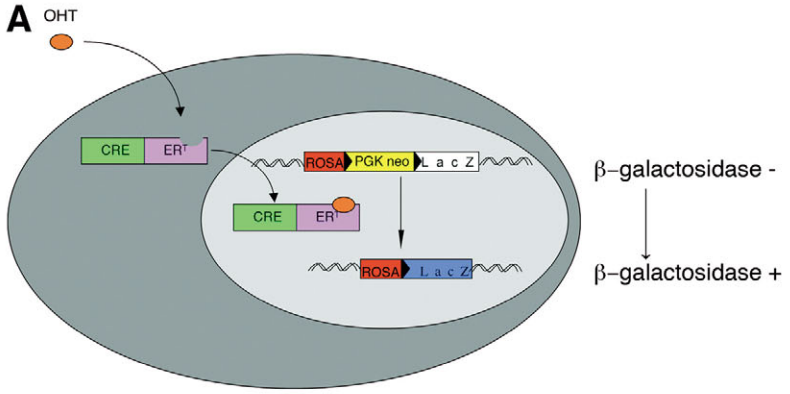

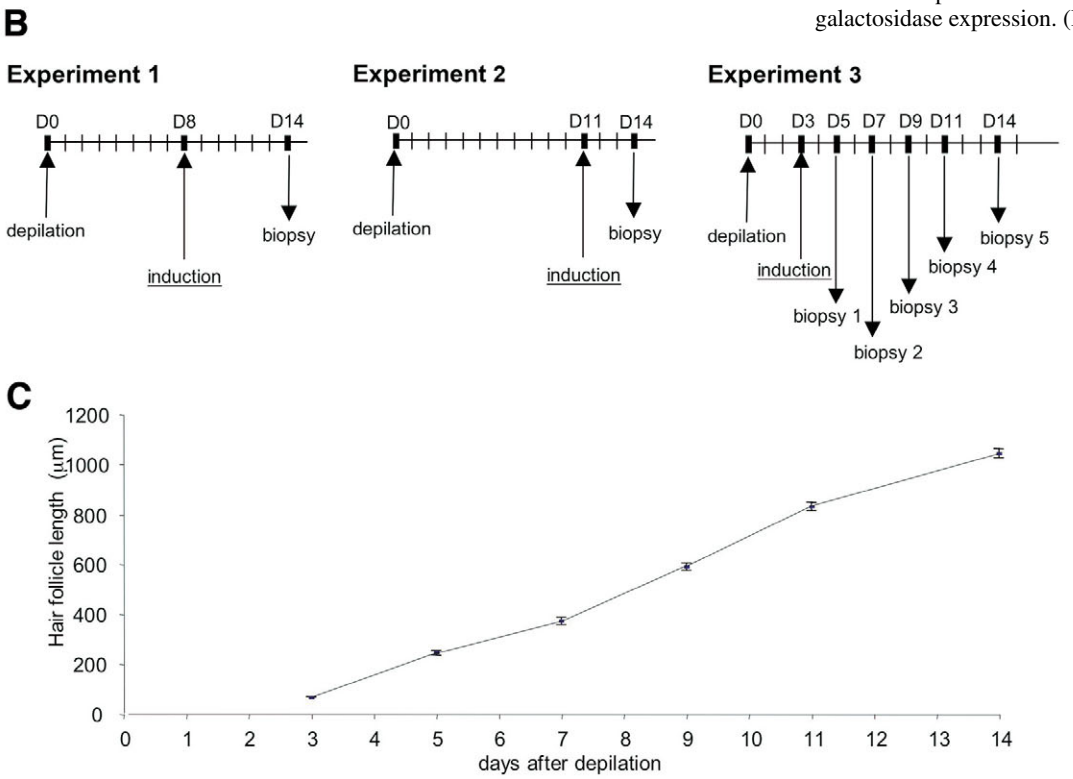

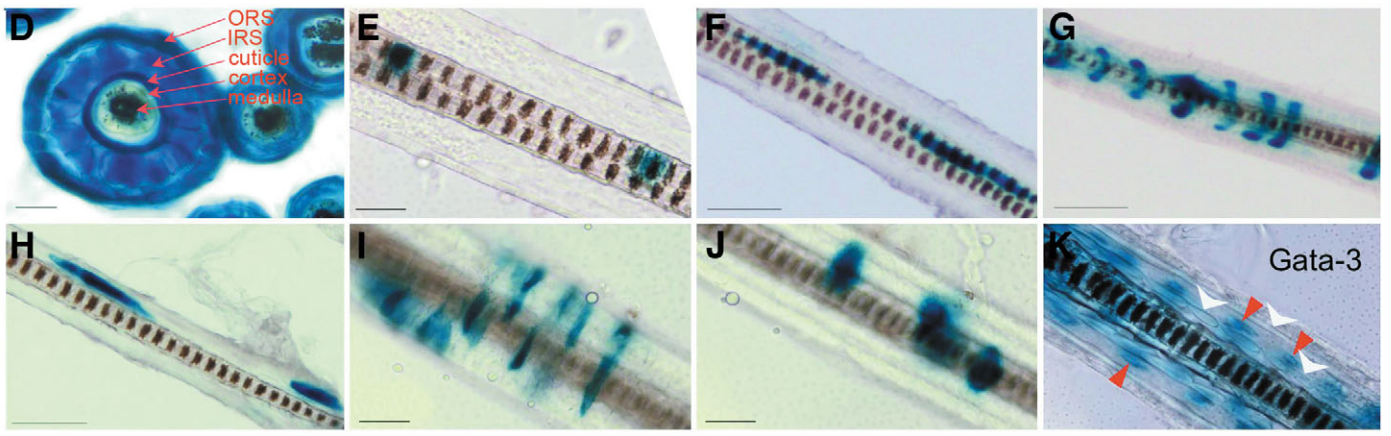

Fig. 1. Experimental design. (A) The method of temporal induction of clones: OHT binds to the mutated estrogen receptor (ER^T) inducing nuclear translocation of CreERT and excision of the LoxP-flanked-stop-sequence, allowing *lacZ* transcription and leading to inheritable β-galactosidase expression. (B) Experiments 1-3: D0, day of depilation; induction, OHT injection on D8 (day 8) in experiment 1, D11 in experiment 2 and D3 in experiment 3. Skin biopsies and observations are as indicated. (C) HF growth is linear. The length of 40 HFs proximodistal axis (*y*-axis) was recorded after depilation (*x*-axis). (D-K) Cell morphologies. (D) Transverse section of ROSA26 HF. (E-K) In toto views of CMV Cre ER^T×R26R F1 HF displaying labeling in medulla (E), cortex (F), hair cuticle (G), IRS (H), ORS (I,J). (K) GATA-3 nls *lacZ* HF; β-galactosidase stains IRS (Huxley and IRS cuticle layers) cell nuclei (red arrowheads). The adjacent hair cuticle and Henlé layers are negative (white arrowheads). Scale bars: 25 μm in D,E,I,J; 50 μm in F-H.

structures undergo self-renewal in the matrix and simultaneously produce differentiated cells, then the corresponding clones must generate labeled cells in the matrix and along the proximodistal axis. Indeed, in experiment 1, most clones restricted to the IRS (Fig. 2A,B), the cuticle (Fig. 2C,D) or the medulla (Fig. 2E) contribute to the matrix (Table 1, Im, Cm and Mm, n=25 compared with I, C, M, n=1) in addition to generating cells along the entire proximodistal axis of the HF (Fig. 2). Therefore, precursor cells in the matrix clearly undergo self-renewal and continually produce IRS, cuticle or medulla cells from the time of clone induction (D8) until observation (D14).

If there is a permanent pool of precursor cells in the matrix during anagen, then we would expect labeled cells to be present at all times in the D14 matrix, even after early induction. Indeed (experiment 3, Fig. 1), 98% of the clones induced at D3 that contribute to either the IRS or cuticle are also present in the matrix (n=20 out of 21).

The IRS, the cuticle and probably the medulla (see below) are therefore produced from permanent pools of restricted cells during anagen.

The permanent precursors produce transient progenitors

In experiment 1, we rarely identified clones restricted to a single inner structure that did not also contribute to the matrix. Such clones would have indicated the existence of transient progenitors. However, this lack of detection may be due to the dynamics of HF growth, in which the most distal cells continually disappear (see Tobin et al., 2002), with only the younger ones remaining. If this is the case, cells produced by a labeled transient progenitor, which has limited contribution to the structure, progressively disappear at the distal part of the HF during the time between induction and observation. Therefore, we investigated whether transient progenitors exist by reducing the interval between induction and observation to only three days (Fig. 1B, experiment 2, induction on D11, observation on D14). As in experiment 1, permanent precursors for each structure are detected (n=16, Table 2 and Fig. 3G-L), but we also detected 24 clones labeled only in the upper part of the HF (Table 2 and Fig. 3A-F). This labeling pattern, found in the IRS (Fig. 3A,B), the cuticle (Fig. 3C,D) or the medulla (Fig. 3E,F), indicates that the labeled cells correspond to subclones of clones produced by permanent precursors. The detection of these subclones demonstrates the existence of transient progenitors for each inner structure of the HF. For the IRS and the cuticle, most instances of labeling (n=4/6 for the IRS and n=6/9 for the cuticle) correspond to two cells (Fig. 3A,B), indicating that the transient progenitor divides only once. For the medulla, the subclones comprise more than two cells, indicating that the medulla progenitors divide more than once before terminal differentiation.

Table 2. Existence of transient progenitors for HF inner structures

Clones labeled in the inner structures	D8	D11
Associated with labeled cells in the matrix	37	16
Non-associated with labeled cells in the matrix	3	24

Transient progenitors and permanent precursors of inner HF structures. The restricted clones have been added (I, C, M, Im, Cm, Mm) to the combined clones with ORS (OI, OC, OM, OIm, OCm, OMm, respectively) as these are issued from double-event of recombination.

Spatial organization of the clonal hierarchy of the matrix cells

The mitotic activity of the HF does not extend beyond the most distal part of the DP (Kobielak et al., 2003; Oshima et al., 2001; Epstein and Maibach, 1965). Both transient progenitors and permanent precursors must therefore lie in this region. To define their relative positions, we determined the position of the most distal labeled cell of the clones induced on D11 (Fig. 4A). Within a given structure, the most distal cell of the clones from transient progenitors is more distal than the most distal cell from the permanent precursors (Fig. 4A). As these clones were induced at the same time, the position of the transient progenitors in the matrix must be more distal than that of the permanent precursors. Hence, a more detailed analysis of labeling in the matrix reveals the complex spatial clonal organization of cells.

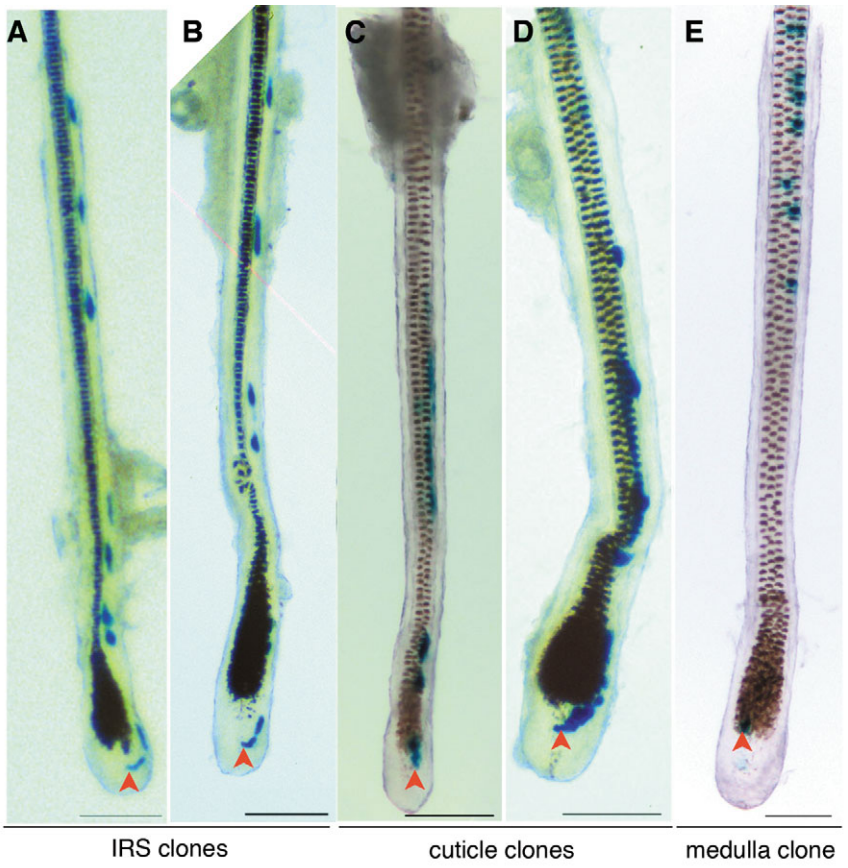

Fig. 2. Inner HF structure clones of permanent precursors. Clones induced on D8 and observed on D14. (A,B) IRS clones; (C,D) cuticle clones; (E) a medulla clone. β-Galactosidase$^+$ cells are present in the matrix. Scale bars: 100 μm.

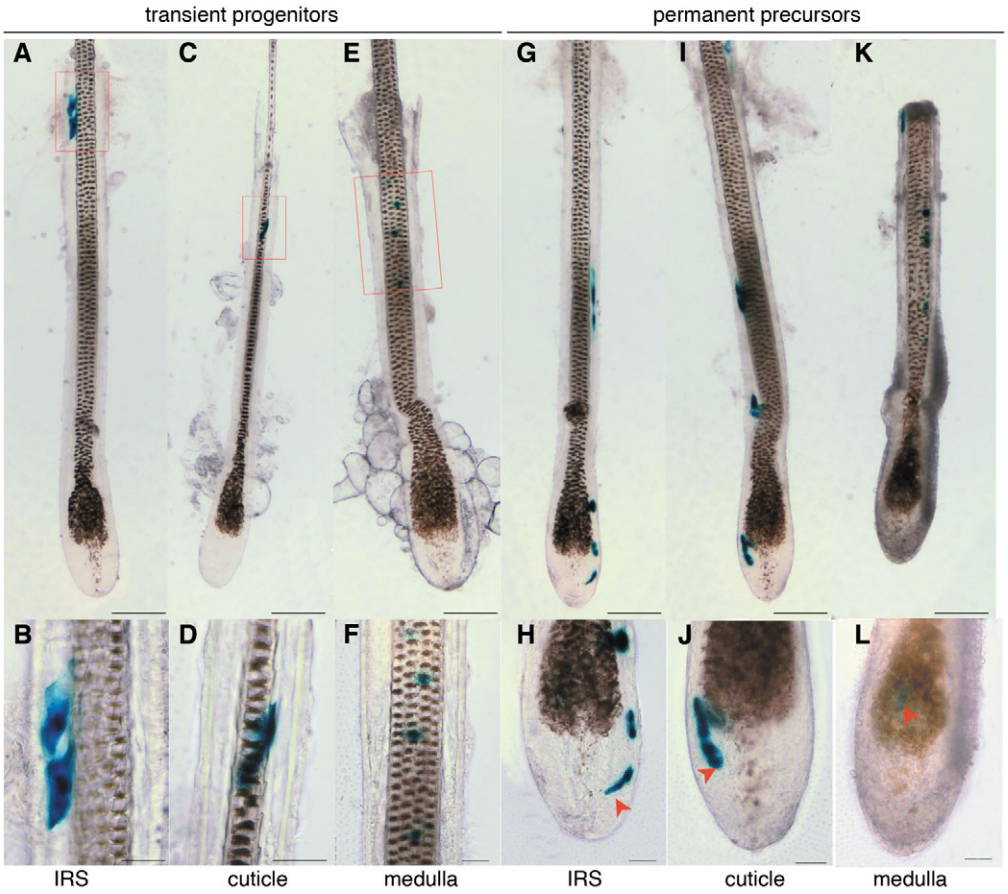

Fig. 3. Inner HF structure clones of transient progenitors. Clones induced on D11 and observed on D14. (A-F) Clones of transient progenitors (absence of labeling in the matrix). The number of labeled cells (in red rectangles) reveals the proliferative potential of the progenitors. (A,B) IRS progenitor divided once. (C,D) Cuticle progenitor divided once. (E,F) Medulla progenitor divided two or three times. (G-L) Clones of permanent precursors (labeled cells in the matrix, arrowheads) in the same experiment. (G,H) IRS; (I,J) cuticle; (K,L) medulla. Scale bars: 100 μm in A,C,E; 25 μm in B,D,F.

IRS clones from permanent precursors display a very stereotyped pattern (Fig. 4B,C; Fig. 3H), whereby two clusters of two cells (marked 1, 2 and 3, 4 in Figs 3 and 4) are aligned along an arc and the most proximal cell is systematically juxtaposed to the DP (cell 1). This pattern is the only pattern observed (in experiments 1 and 2, Im, n=18, Table 1), demonstrating that permanent precursors occupy only one position in the matrix. As permanent precursors occupy a more proximal position than transient progenitors (Fig. 4A), the cell juxtaposed to the DP – the most proximal labeled cell – is therefore the permanent precursor. Thus, the clonal hierarchy is as follows: cell 1 juxtaposed to the DP is the permanent precursor; it undergoes self-renewal and produces cell 2 (the transient progenitor), which is not juxtaposed to the DP; cell 2 produces cells 3 and 4 by symmetric division; cells 3 and 4 are post-mitotic and differentiate. Interestingly, cells 3 and 4 remain attached to each other throughout their movement towards the more distal part of the HF (Fig. 3G,H and Fig. 4B-D).

Cuticle clones also have a unique, stereotyped pattern in the matrix (in experiments 1 and 2, Cm, n=10, Fig. 4E,F and Fig. 3J, Table 1) displaying a permanent precursor juxtaposed to the DP and the transient progenitor is in the second layer of matrix cells. Finally, there are medulla clones from permanent precursors that have labeled cells in the matrix close to the DP (Fig. 4G and Fig. 3L) and medulla clones from transient progenitors (Fig. 3F). Therefore, the cuticle and the medulla are clearly produced in a similar manner to the IRS.

Thus, the precursors of each inner structure of the HF are all located in the cell layer juxtaposed to the DP. This layer is therefore a germinative layer, given that the precursors of the inner structures are permanent during anagen, they self-renew themselves, they produce transient progenitor exhibiting different properties, presumably by asymmetric division, they are stem of more differentiated cells and their position near the DP may correspond to a niche. Thus, they can be identified as stem cells.

Inner structures are organized into proximodistal clonal columns

Within each inner structure, clones were organized into proximodistal columns. We did not observe cellular intercalation between adjacent columns around the circumference. This applies to all cells of a clone, from the cell juxtaposed to the DP in the matrix to the most distal cell, and to all categories – the IRS (Fig. 2A,B and Fig. 3G,H, Im, n=18, experiments 1 and 2, Table 1) and cuticle (Fig. 2C,D and Fig. 3I,J, Cm, n=10, experiments 1 and 2, Table 1) and, with one exception, the medulla (Fig. 2E and Fig. 3K,L, n=3/4).

Each column was clearly formed from several stem cells because unlabelled cells were invariably intercalated with labeled ones. Columns therefore have a polyclonal origin. We calculated the size of the polyclone at the origin of each column of the inner structures of the HF, using the medial participation of founder cells method whereby the number of founder cells corresponds to the total HF length divided by the fraction of the HF proximodistal axis to which a clone participates. The calculation indicates that IRS and cuticle columns are

A

Position of the most distal cell of D11 clones along the P-D axis (μm)

origin of labelled cells	IRS	cuticle	medulla
permanent precursor	588 (+/-16) (n=10)	464 (+/-48) (n=4)	474 (+/-55) (n=3)
transient progenitor	800 (+/-22) (n=8)	669 (+/-19) (n=4)	536 (+/-62) (n=3)

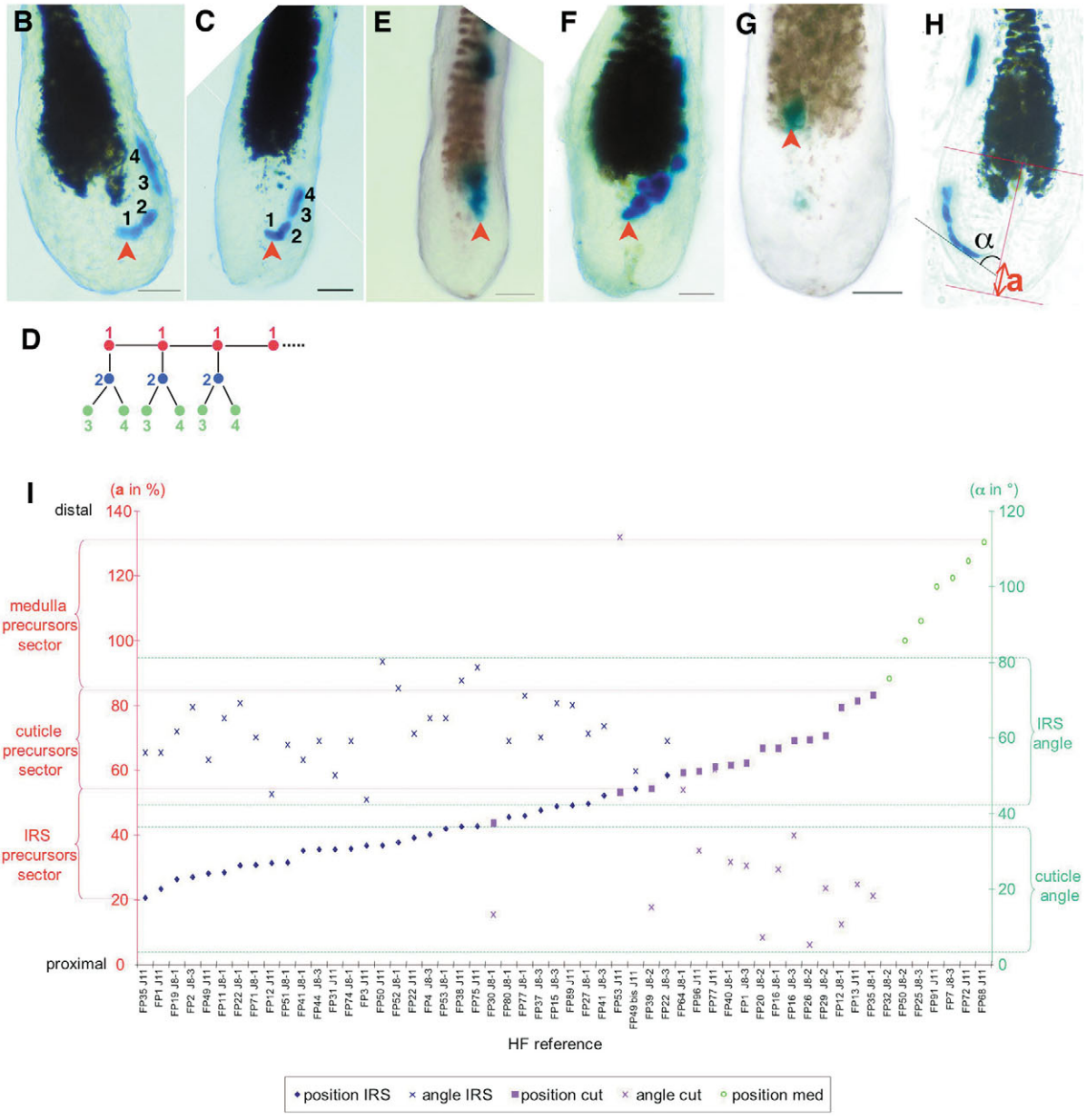

Fig. 4. The permanent precursors of the inner structures are organized into distinct sectors and are arranged with different orientations after division. (A) Position of the most distal cell (in μm) in the clones induced at D11. This position is more distal for clones produced by transient progenitors than for clones produced by permanent precursors. (B,C,E-G) In toto views of the matrix. Same clones as in Fig. 2. Arrowheads indicate the cell juxtaposed to the DP. Scale bars: 25 μm. (B,C) IRS clones showing two related pairs of cells (1, 2 and 3, 4) and progressive intercalation of β-galactosidase$^+$ cells between the pairs in layer 3 (see Fig. 6). 1, permanent precursor; 2, transient progenitor; 3,4, cells originating from division of the progenitor (see text); (D) Diagram of IRS mode of growth. (E,F) Cuticle clones; (G) A medulla clone. (H) Measurement of the position (a) of the permanent precursor and of the angle of the alignment of the permanent precursor and the transient progenitor (α) with respect to the proximodistal axis of the DP. (I) position (*y*-axis, in % of the length of the proximodistal axis of the DP, 'a' value in H) of the permanent precursors of the IRS (blue lozenge), cuticle (pink square), medulla (green circle). *y*-axis is the value (in degrees) of α in G of the IRS (blue cross) and the cuticle (pink cross). *x*-axis gives the clone reference (from experiments 1 and 2).

generated by four stem cells, and the medulla columns by about six cells (data not shown). We argued previously that the stem cell is attached to the DP, and this, together with the strict columnar organization of clones, argues that the precursors for each column are aligned along the proximodistal axis of the DP. The IRS, cuticle and medulla, are thus formed from proximodistal columns that are polyclonal in origin. This organization necessarily demands the controlled intercalation of cells produced by the transient progenitors.

Stem cells are organized into several exclusive proximodistal sectors

The stem cells at the origin of the various structures of the HF could be organized in several different ways. To distinguish among them, we calculated the position of each stem cell along the proximodistal axis of the DP (Fig. 4H). This position is expressed as a percentage of the length of the proximodistal axis of the DP up to the bulb, which hides the upper part of the DP, such that a graphic representation can be drawn independently of small differences in the size of the matrix (Fig. 4I). This representation indicates that the stem cells for the various structures occupy different, and mutually exclusive sectors. A proximal sector (25±5% to 56±2.5%) corresponds to the stem cells for the IRS, an intermediate sector (56±2.5% to 85%) corresponds to the stem cells for the cuticle, and a distal sector (85% to 130%) corresponds to stem cells for the medulla. The observed indetermination between sectors corresponds to about one cell diameter (6,3% of the length of the proximal-distal axis). As each stem cell contributes to a single proximodistal column, the formation of a complete concentric layer necessitates the participation of all cells in the matrix in the circumferential dimension. Therefore, each sector occupies the whole circumference in the matrix.

We determined the number of cells in each sector, by measuring the percentage of the proximodistal axis on an optical section of a matrix in which the cell membranes were marked with green fluorescent protein (GFP). The IRS and cuticle sectors each contained four cells, and we estimated that the medulla sector, where the labeling was not clear enough to draw cell contour, contains five or six cells (Fig. 6).

As the cells aligned along the proximodistal axis of the DP are at the origin of a single column in each concentric layer, they should constitute the polyclone at the origin of the column. Their number must therefore be equal to the size of the polyclone. This was indeed the case for the IRS and the cuticle: the number of cells in the sectors along this dimension (four cells) was identical to the calculated size of the polyclone at the origin of the columns (four cells).

Thus, globally, the stem cells are organized in exclusive sectors around the circumference of the central DP. The cells within a given sector share the same fate. We also identified the proximal sector (0-25±5%) as a sector containing cells that do not participate in any of the inner structures of the HF.

The organization of the HF inner structures in concentric layers is prefigured in the matrix

The production of concentric layers of the HF by cells organized in sectors along the proximodistal axis of the matrix raises the possibility that HF organization is prefigured in the organization of the matrix. However, projection of the organization of cells along the proximodistal axis in the matrix to their organization in concentric layers along a perpendicular axis would require a rotation involving a cellular strategy. We investigated whether the spatial arrangement of the cells after the division of the permanent precursors was part of this strategy.

In the IRS sector, the alignment of the permanent precursor and the transient progenitor form an angle of 63° with respect to the proximodistal axis of the matrix (Fig. 4I). The corresponding angle is only 20° for cells in the cuticle sector (Fig. 4I). We found that this angle depends on the sector, given that it is constant for all cells within a given sector but differs considerably between sectors (Fig. 4I; data not shown). The fixation of this angle may be part of the strategy involved in orienting cells, from their production near the DP to their final location in the upper part of the HF.

Globally this orientation is a parameter defined by the sector to which these cells belong. Differences between cells from different sectors are to be added to the specific parameters of proliferation and intercalation revealed by clonal patterns (see above). At least some of these characteristics are probably intrinsic, suggesting that the cells of the different sectors are programmed differently.

The mode of production of ORS cells

The ORS, like other HF structures, grows from restricted precursors during anagen (Table 1). However, ORS clones differ radically from inner structure clones in other properties. The labeling induced on D8 and observed on D14 is surprisingly heterogeneous in distribution (Fig. 5A-D). The clonal complexity index [the number of clones that participate to an elementary region (Petit et al., 2005)] (Fig. 5N) shows a maximum of 13, which represents only 22% of the clones. Therefore, the analysis of clonal complexity index failed to identify a family of clones systematically contributing to one region of the HF. These data suggest that ORS progenitors are dispersed throughout the structure and that there is no pool of permanent stem cells at the origin of the ORS. They suggest instead a mode of coherent growth, consistent with the observed systematic arrangement of the labeled cells in coherent clusters (Fig. 5A-D).

Clone size (cell number) and clonal extension were extremely disparate (Fig. 5O,P). This indicates that the cells labeled on D8 do not have an equivalent outcome. These differences may be due to differences in generation time, division potential or apoptosis. If only differences in generation time and/or division potential were involved, then the number of ORS clones would remain constant during anagen. We tested this hypothesis (Fig. 1B, experiment 3). Remarkably, 70% of the labeling observed on D9 had disappeared by D14 (Fig. 5Q). This decrease in labeling indicates that a large fraction of ORS cells undergo apoptosis, leading to the eventual disappearance of many clones. To test this point directly, we have performed an immunostaining against cleaved caspase 3 on cryostat sections of HF in anagen. We have detected apoptotic cells in the ORS (Fig. 5E-M). We investigated whether this apoptosis specifically affected certain regions of the ORS by analyzing the distribution of clones as a function of their size (Fig. 5O). Regardless of cell number (1 to 121) the clones were evenly distributed in the HF (Fig. 5N) and we therefore found no evidence for preferential regional apoptosis of ORS cells.

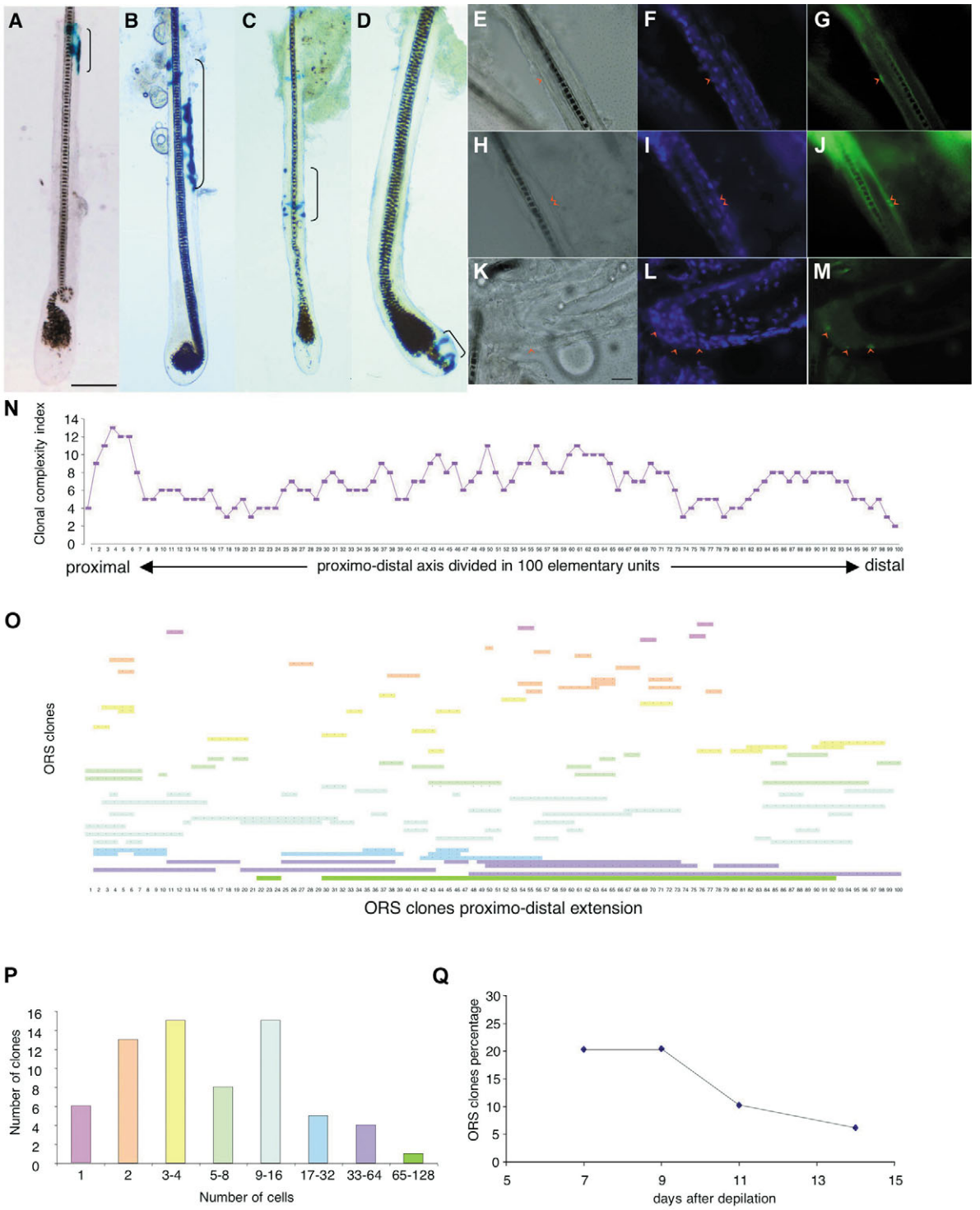

Fig. 5. The ORS follows a coherent regional mode of growth and shows apoptosis. (A-D) In toto views of ORS clones; ORS precursors are dispersed (brackets) along the proximodistal axis of the HF. Scale bar: 100 μm. (E-M) Anti-cleaved caspase 3 immunostaining on 20 μm anagen HF sections. Scale bar: 25 μm. (E,H,K) Bright field. (F,I,L) DAPI staining in blue. (G,J,M) Cleaved caspase 3 staining in green. Apoptotic cells are marked by red arrowheads. (N) Clonal complexity (*y*-axis) of the 100 subdivisions of equal length of the ORS proximodistal axis (*x*-axis). Clonal complexity is the number of times a subdivision is labeled (calculated from the 60 clones in O, Experiment 1). (O) Classification of the 60 ORS clones according to their proximodistal extension. Each horizontal line corresponds to a clone (the colored rectangles). The numbers indicate the position of the clone according to the subdivision of the proximodistal axis in 100 equal parts. Each color refers to the number of cells in the clone. See color code in P. (P) Number of clones in relation to the number of β-galactosidase$^+$ cells. The *x*-axis represents the number of β-galactosidase$^+$ cells for each class of clones. The *y*-axis represents the number of clones. ORS clones differ considerably in size. (Q) Percentage of ORS clones of the total number of HFs observed (labeled and unlabeled) (*y*-axis) calculated for D7, D9, D11 and D14 (experiment 3). Percentage decrease indicates the loss of ORS clones during anagen owing to apoptosis.

Thus, unlike other HF structures, the ORS is clearly produced from progenitors with uneven growth properties rather than from stem cells. We investigated the possible polyclonal origin of the ORS by analyzing clones induced before the onset of anagen. HF from the animal used in experiment 1 were observed after one additional cycle of hair renewal (hair was removed again 26 days after the initial depilation). Both labeled and unlabeled cells contribute to the structure of the ORS (70 of 70 observations, data not shown). Thus, like other HF structures, the ORS has a polyclonal origin.

The ORS therefore differs from the IRS, cuticle and medulla as it follows a regional, coherent mode of growth from progenitors of polyclonal origin and the proliferation of these progenitors is limited by apoptosis. Apoptosis affects all progenitors, whatever their position in the ORS, but the clones are affected to different extents. Overall the ORS remains somewhat static with a balance between apoptosis and mitosis.

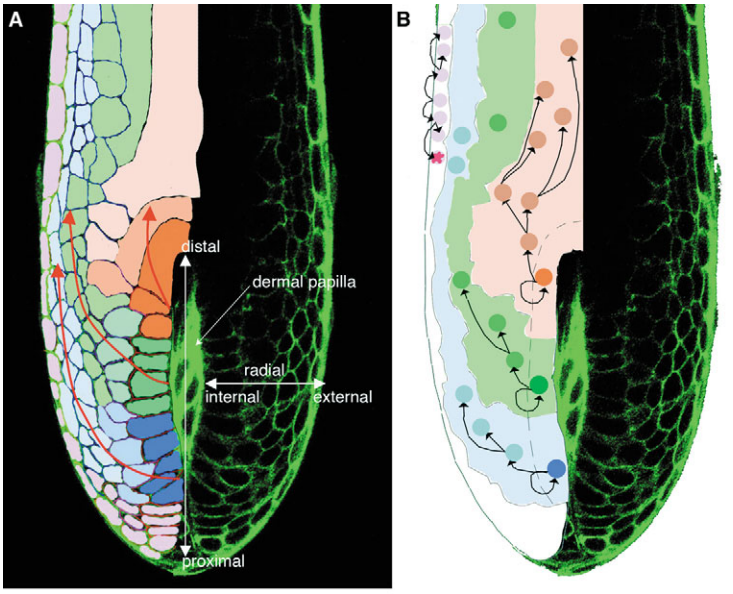

Fig. 6. Cell behavior and cell fate organization in the HF matrix. The hypothesis of behavior and fate uncoupling. (A) Cell outlines were drawn from an optical confocal section of a HF from a farnesylated-GFP transgenic mouse in which GFP labels the cell membranes. The right side is the mirror image of the picture of the optical confocal slice. Cell behaviors are organized along the radial dimension of the matrix: the stem cells form a germinative layer juxtaposed to the DP (darkest colors). They undergo self-renewal and generate the transient progenitors in the second layer (in lighter colors). The next layers contain the postmitotic cells (lightest colors) that intercalate to produce columns. Cell fates are assigned according to the position of the stem cells along the proximodistal axis. Each structure is produced by several cells forming a sector. The most proximal cells are not involved in the formation of any inner structure; they are clonally related to the ORS (pink) (data not shown). Within a sector, the stem cells and the transient progenitors form a characteristic angle (63° for the IRS and 20° for the cuticle). This organization of matrix cells prefigures the organization of the HF in concentric layers (red arrows). Cell fates and cell behaviors therefore seem to be uncoupled and organized in two orthogonal systems. (B) Clonal hierarchy in the matrix (see text).

Discussion

A model of HF growth based on a map of the fate and behaviors of matrix cells

From the results presented above, we can generate a map of the fate and behaviors of matrix cells (Fig. 6). In the radial dimension, the matrix is divided into several layers, including the germinative layer (stem cells, darkest colors), progenitor layer (lighter colors) and post-mitotic layers (lightest colors) (Fig. 6). In the proximodistal dimension, the germinative layer comprises three sectors that contain the stem cells for the IRS (blue), the cuticle (green) or the medulla (orange). The proximodistal order of stem cells in the matrix corresponds to the order of the concentric cell layers in the HF, from the most peripheral (the IRS) to the innermost (the medulla) structure. The most proximal sector (pink) is not involved in the formation of the inner structures. It is clonally related to the ORS.

Altogether, this map of the fate and behavior explains the complex morphology of the HF in terms of a few operations controlled and executed in the matrix: (1) an absence of circumferential intercalation within and above the matrix, resulting in the organization of the HF into proximodistal columns; (2) an intercalation in the matrix of the cells produced by the transient progenitors that accounts for the polyclonal origin of these columns; (3) an arrangement of cells after stem cell division that relates to the rotation that converts the proximodistal axis in the matrix to the radial axis in the HF; and (4) an absence of radial intercalation in the matrix that maintains the organization in concentric layers. As a consequence of these cell operations, the proximodistal sectors in the germinative layer prefigure the radial order of the inner concentric layers of the HF.

This fate map bridges the gap in our knowledge regarding the way in which multipotent epithelial stem cells in the bulge renew the multi-tissue HF. The remaining missing step is how the multipotent epithelial stem cells diversify when the matrix reforms. This step can be analyzed further by using the method of clonal analysis presented in this study.

Formation of the outer layer and coordination of the growth of inner and outer cell layers

Our results show that the ORS is a very special structure that differs from the IRS, the cuticle and the medulla. Its precursor cells are not permanent, do not occupy a specific niche and their lineages are not stereotyped. The outer layer of the HF is polyclonal in origin and displays regional growth. It is produced by progenitors dispersed throughout the ORS that display coherent growth and apoptosis. This is consistent with Ki67 labeling, which demonstrated the dispersal of proliferating ORS cells throughout the layer (Kobielak et al., 2003). However, our results indicate that the ORS does not have a simple proliferative mode of growth. The progressive disappearance of labeling during anagen and the presence of cleaved caspase 3-positive cells (Fig. 5E-M) demonstrate the involvement of apoptosis. Furthermore, variably sized clones generated on the same day suggest that some are more sensitive to apoptosis than others. In *Drosophila*, cell competition plays a central role in controlling the growth and size of epithelia (Simpson, 1979). This cell competition involves super

competitor clones that grow at the expense of less competitive ones, which undergo apoptosis (Moreno et al., 2002). In the ORS, many of these elements are present: cell death, very large clones (possibly super competitors) and variable clone sizes, which may reflect heterogeneity in susceptibility to cell death. If cell competition is indeed at work in ORS morphogenesis, this would constitute the first demonstration of this complex process in vertebrates and would raise the possibility of a ancestral and fundamental role of cell competition in the biology of epithelia.

The HF has a linear growth (Fig. 1B) that fits with the stem cell mode of growth of the IRS, cuticle and medulla that progress in concert during the entire duration of anagen. However, this linear growth does not fit with a simple proliferative mode of growth of the ORS. Therefore the non-regional apoptosis detected in the ORS probably adapts the growth of the outer layer to the linear growth of the inner layers of the HF by modulating a proliferative mode of growth that gives an exponential increase in cell number. This coordination is essential for balanced HF morphogenesis.

The organizations in the matrix

Radial organization of cell behaviors

Our results confirm the view that the matrix is the only proliferative region of the inner structures of the HF. However, they show that the matrix is not composed of equivalent cells, a finding that complements the results of Kopan and collaborators (Kopan et al., 2002). We also show that each HF inner structure is produced by two categories of precursors: permanent precursors with attributes of stem cells [self-renewal, asymmetric division and their location in the germinative layer, whose proximity with the DP provides a specific micro-environment that may constitute a niche (Fuchs et al., 2004)] and transient progenitors that divide symmetrically and produce postmitotic cells (Fig. 6B). Their lineage is highly stereotyped. In this study, we were able to locate the three types of cells in the matrix, including the permanent precursor cells that are juxtaposed to the DP (the germinative layer), the transient progenitors that are in the next radial layer and the postmitotic cells, which exist in the layers. Clonal analysis also revealed intercalation of the postmitotic cells, at the level of the more external layers. This intercalation applies to the IRS, the cuticle and the medulla. It will be interesting to determine which type of intercalation is involved. Radial and mediolateral intercalation types are used several times during vertebrate development, for example for gastrulation movements, and they rely on different basic mechanisms (Keller, 2002). Whatever the case may be, cell behavior (symmetric or asymmetric division, intercalation, and probably adhesion and cell polarity) are organized radially in the HF matrix.

Interestingly, several molecular markers and signaling patterns have been shown to vary across the radial plane. Lef1 and Tcf3, two transcription factors activated by the canonical Wnt pathway, are expressed close to the DP (probably in the first two layers) (Jamora et al., 2003) and in the outer cell layer (DasGupta and Fuchs, 1999), respectively. The adhesion molecule P-cadherin is found in the cells closest to the DP (layers 1 and 2) and E-cadherin is found in the more external layers. The genetic circuitry controlling this differential expression of cadherins has been identified: Noggin secreted by the DP inhibits BMP, inducing the production of Lef1, which represses E-cadherin in the layers near the DP (Jamora et al., 2003). The shift from one type of cadherin to another may be involved in the control of cell intercalation, as maybe the non-canonical Wnt pathway (reviewed by Myers et al., 2002).

Thus, both cell behaviors and the genetic markers probably involved in their control are organized radially. The DP may be responsible for this organization. For example, a radial gradient of BMPs may be established as a result of the homogeneous expression of Noggin in the DP. The relationship between cell behavior, signaling pathways in the matrix and the DP and other molecular aspects remains to be elucidated. However, the radial dimension seems to correspond to the control of many cellular behaviors, regardless of the cell fate.

Proximodistal organization of cell fates

Several analyses have suggested the existence of different precursors in the matrix (Ghazizadeh and Taichman, 2001; Kamimura et al., 1998; Kopan et al., 2002; Kulessa et al., 2000). Our analysis demonstrates the existence of three distinct sectors in the matrix corresponding to IRS precursors, precursors for the cuticle and the cortex and precursors for the medulla. These sectors are organized along the proximodistal axis in the germinative layer. Wnt activity, revealed by a Wnt reporter gene (TOPGAL), located hair shaft precursors in the distal part of the matrix (DasGupta and Fuchs, 1999). Our clonal analysis is consistent with these findings. We demonstrated that the structure to which a precursor contributes depends on its proximodistal position. In the fate map, we suggest that the hair shaft (medulla, cortex and cuticle) is produced by cells more distal than those that produce the IRS. These sectors probably remain static after their establishment at the beginning of anagen because over the longest observable periods, a labeled stem cell produces only one type of differentiated cell. The strict proximodistal organization of the germinative layers into sectors raises the possibility that the cells of these sectors are different. These sectors cannot be differentiated with known biochemical markers, but do differ in the cell arrangement after the permanent precursor division.

Thus, there are at least three different populations of stem cells in the matrix, in terms of properties, location and, most importantly, fate. We suggest that the proximodistal axis of the matrix corresponds to the organization of stem cell fate. Cell fates and cell behaviors therefore seem to be uncoupled and are probably organized by means of two orthogonal systems.

Conclusion: the uncoupling of developmental operations

In summary, the matrix seems to be organized by two systems working in orthogonal dimensions and controlling two key operations of HF morphogenesis, notably cell diversification and cell behavior. This combination of two systems, exploiting the three dimensions of the matrix, might have greatly simplified evolution of the morphogenetic strategy used to create HFs and to diversify them (Wu et al., 2004) in mammals. The basis of this simplification is the uncoupling of cell diversification and morphogenesis suggested by the fact that the same cell behavior (for instance a stem cell mode of division) is shared by cells with different fate (IRS, cuticle and

medulla precursors). The HF matrix thus provides a paradigm for elucidating more complex embryonic structures in which the existence of three dimensions may have made it possible to uncouple various developmental operations, thereby considerably simplifying their evolution.

We thank Estelle Hirsinger, Anne-Cécile Petit, Shahragim Tajbakhsh, Elena Tzouanacou and Valerie Wilson for their comments on the manuscript; Daniel Metzger for the CMV Cre ER^t mice and Philippe Soriano for the R26R mice; Alexander Medvinsky for the a-EGFP mice; Franck Grosveld for the GATA-3 nls *lacZ* mice; Pascal Roux for assistance with confocal imaging; Suzanne Capgras, Clémire Cimper and Pascal Dardenne for technical assistance; and Christine Mariette for ROSA26 sections. This work was supported by grants from Cells into Organs (EU Framework 6 project LSHM-CT-2003-504468), EurostemCell (EU Framework 6 project LHSB-CT-2003-503005), GPH Stem cells (Institut Pasteur), ARC (Association pour la Recherche sur le Cancer) and AFM (Association Française contre les Myopathies). J.F.N. is from the Institut National de la Recherche Médicale (INSERM).

References

Alonso, L. and Fuchs, E. (2003). Stem cells in the skin: waste not, Wnt not. *Genes Dev.* **17**, 1189-1200.

Botchkarev, V. A. (2003). Bone morphogenetic proteins and their antagonists in skin and hair follicle biology. *J. Invest. Dermatol.* **120**, 36-47.

Cotsarelis, G., Sun, T. T. and Lavker, R. M. (1990). Label-retaining cells reside in the bulge area of pilosebaceous unit: implications for follicular stem cells, hair cycle, and skin carcinogenesis. *Cell* **61**, 1329-1337.

DasGupta, R. and Fuchs, E. (1999). Multiple roles for activated LEF/TCF transcription complexes during hair follicle Development and differentiation. *Development* **126**, 4557-4568.

Epstein, W. L. and Maibach, H. I. (1965). Cell renewal in human epidermis. *Arch. Dermatol.* **92**, 462-468.

Feil, R., Brocard, J., Mascrez, B., LeMeur, M., Metzger, D. and Chambon, P. (1996). Ligand-activated site-specific recombination in mice. *Proc. Natl. Acad. Sci. USA* **93**, 10887-10890.

Fuchs, E., Merrill, B. J., Jamora, C. and DasGupta, R. (2001). At the roots of a never-ending cycle. *Dev. Cell* **1**, 13-25.

Fuchs, E., Tumbar, T. and Guasch, G. (2004). Socializing with the neighbors: stem cells and their niche. *Cell* **116**, 769-778.

Gambardella, L., Schneider-Maunoury, S., Voiculescu, O., Charnay, P. and Barrandon, Y. (2000). Pattern of expression of the transcription factor Krox-20 in mouse hair follicle. *Mech Dev.* **96**, 215-218.

Ghazizadeh, S. and Taichman, L. B. (2001). Multiple classes of stem cells in cutaneous epithelium: a lineage analysis of adult mouse skin. *EMBO J.* **20**, 1215-1222.

Hardy, M. H. (1992). The secret life of the hair follicle. *Trends Genet.* **8**, 55-61.

Hendriks, R. W., Nawijn, M. C., Engel, J. D., van Doorninck, H., Grosveld, F. and Karis, A. (1999). Expression of the transcription factor GATA-3 is required for the Development of the earliest T cell progenitors and correlates with stages of cellular proliferation in the thymus. *Eur. J. Immunol.* **29**, 1912-1918.

Jamora, C., DasGupta, R., Kocieniewski, P. and Fuchs, E. (2003). Links between signal transduction, transcription and adhesion in epithelial bud development. *Nature* **422**, 317-322.

Kamimura, J., Lee, D., Baden, H., Brissette, J. and Dotto, G. (1998). Primary mouse keratinocyte cultures contain hair follicle progenitor cells differentiation potential. *J. Invest. Dermatol.* **109**, 534-540.

Kassar-Duchossoy, L., Giacone, E., Gayraud-Morel, B., Jory, A., Gomes, D. and Tajbakhsh, S. (2005). Pax3/Pax7 mark a novel population of primitive myogenic cells during development. *Genes Dev.* **19**, 1426-1431.

Kaufman, C. K., Zhou, P., Pasolli, H. A., Rendl, M., Bolotin, D., Lim, K. C., Dai, X., Alegre, M. L. and Fuchs, E. (2003). GATA-3: an unexpected regulator of cell lineage determination in skin. *Genes Dev.* **17**, 2108-2122.

Keller, R. (2002). Shaping the vertebrate body plan by polarized embryonic cell movements. *Science* **298**, 1950-1954.

Kobielak, K., Pasolli, H. A., Alonso, L., Polak, L. and Fuchs, E. (2003). Defining BMP functions in the hair follicle by conditional ablation of BMP receptor IA. *J. Cell Biol.* **163**, 609-623.

Kopan, R., Lee, J., Lin, M. H., Syder, A. J., Kesterson, J., Crutchfield, N., Li, C. R., Wu, W., Books, J. and Gordon, J. I. (2002). Genetic mosaic analysis indicates that the bulb region of coat hair follicles contains a resident population of several active multipotent epithelial lineage progenitors. *Dev. Biol.* **242**, 44-57.

Kulessa, H., Turk, G. and Hogan, B. L. (2000). Inhibition of Bmp signaling affects growth and differentiation in the anagen hair follicle. *EMBO J.* **19**, 6664-6674.

Langbein, L. and Schweizer, J. (2005). Keratins of the human hair follicle. *Int. Rev. Cytol.* **243**, 1-78.

Ma, L., Liu, J., Wu, T., Plikus, M., Jiang, T. X., Bi, Q., Liu, Y. H., Muller-Rover, S., Peters, H., Sundberg, J. P. et al. (2003). 'Cyclic alopecia' in Msx2 mutants: defects in hair cycling and hair shaft differentiation. *Development* **130**, 379-389.

Merrill, B. J., Gat, U., DasGupta, R. and Fuchs, E. (2001). Tcf3 and Lef1 regulate lineage differentiation of multipotent stem cells in skin. *Genes Dev.* **15**, 1688-1705.

Moreno, E., Basler, K. and Morata, G. (2002). Cells compete for decapentaplegic survival factor to prevent apoptosis in Drosophila wing development. *Nature* **416**, 755-759.

Morris, R. J., Liu, Y., Marles, L., Yang, Z., Trempus, C., Li, S., Lin, J. S., Sawicki, J. A. and Cotsarelis, G. (2004). Capturing and profiling adult hair follicle stem cells. *Nat. Biotechnol.* **14**, 14.

Muller-Rover, S., Handjiski, B., van der Veen, C., Eichmuller, S., Foitzik, K., McKay, I. A., Stenn, K. S. and Paus, R. (2001). A comprehensive guide for the accurate classification of murine hair follicles in distinct hair cycle stages. *J. Invest. Dermatol.* **117**, 3-15.

Myers, D. C., Sepich, D. S. and Solnica-Krezel, L. (2002). Convergence and extension in vertebrate gastrulae: cell movements according to or in search of identity? *Trends Genet.* **18**, 447-455.

Niemann, C. and Watt, F. M. (2002). Designer skin: lineage commitment in postnatal epidermis. *Trends Cell. Biol.* **12**, 185-192.

Oliver, R. F. (1966). Whisker growth after removal of the dermal papilla and lengths of follicle in the hooded rat. *J. Embryol. Exp. Morphol.* **15**, 331-347.

Oro, A. E. and Higgins, K. (2003). Hair cycle regulation of Hedgehog signal reception. *Dev. Biol.* **255**, 238-248.

Oshima, H., Rochat, A., Kedzia, C., Kobayashi, K. and Barrandon, Y. (2001). Morphogenesis and renewal of hair follicles from adult multipotent stem cells. *Cell* **104**, 233-245.

Pan, Y., Lin, M. H., Tian, X., Cheng, H. T., Gridley, T., Shen, J. and Kopan, R. (2004). gamma-secretase functions through Notch signaling to maintain skin appendages but is not required for their patterning or initial morphogenesis. *Dev. Cell* **7**, 731-743.

Petiot, A., Conti, F. J., Grose, R., Revest, J. M., Hodivala-Dilke, K. M. and Dickson, C. (2003). A crucial role for Fgfr2-IIIb signalling in epidermal development and hair follicle patterning. *Development* **130**, 5493-5801.

Petit, A. C., Legué, E. and Nicolas, J. F. (2005). Methods in clonal analysis and applications. *Reprod. Nutr. Dev.* **45**, 321-339.

Shang, L., Pruett, N. D. and Awgulewitsch, A. (2002). Hoxc12 expression pattern in developing and cycling murine hair follicles. *Mech. Dev.* **113**, 207-210.

Simpson, P. (1979). Parameters of cell competition in the compartments of the wing disc of Drosophila. *Dev. Biol.* **69**, 182-193.

Soriano, P. (1999). Generalized lacZ expression with the ROSA26 Cre reporter strain. *Nat. Genet.* **21**, 70-71.

Stenn, K. S. and Paus, R. (2001). Controls of hair follicle cycling. *Physiol. Rev.* **81**, 449-494.

Tobin, D. J., Foitzik, K., Reinheckel, T., Mecklenburg, L., Botchkarev, V. A., Peters, C. and Paus, R. (2002). The lysosomal protease cathepsin L is an important regulator of keratinocyte and melanocyte differentiation during hair follicle morphogenesis and cycling. *Am. J. Pathol.* **160**, 1807-1821.

Tumbar, T., Guasch, G., Greco, V., Blanpain, C., Lowry, W. E., Rendl, M. and Fuchs, E. (2004). Defining the epithelial stem cell niche in skin. *Science* **303**, 359-363.

Wu, P., Hou, L., Plikus, M., Hughes, M., Scehnet, J., Suksaweang, S., Widelitz, R., Jiang, T. X. and Chuong, C. M. (2004). Evo-Devo of amniote integuments and appendages. *Int. J. Dev. Biol.* **48**, 249-270.